Development of Solid Propellant Motor For Low Altitude Model Rockets

Abstract This paper describes the design, analysis, and testing of a solid propellant rocket motor designed to propel a model rocket to an apogee of 50 meters. The motor and the propulsion system had to be integrated into an airframe with a small payload thus had to provide enough thrust to reach the desired altitude yet remain compact and lightweight. All this had to be done with the constraint of only using locally sourced materials.

OpenMotor software was used in simulating the motor performance of the motor. ANSYS Fluent was used to analyze the flow within the motor chamber and nozzle. Data from static tests are presented in this paper for the different motor designs and fuels tested. Sugar was used as fuel in the rocket motor with variations being made on the sugar types: Sucrose and Dextrose. The oxidizer used was Potassium nitrate. The paper presents a comparison of the different fuels used as well as the methods used in the preparation.

The selected motor was able to produce an average thrust of 35 Newtons with a peak thrust of 48 Newtons, which was able to propel the rocket to an apogee of 34 meters.

Keywords Solid propellant, static fire test, thrust curve.

1. Introduction

Rocket launches are a common scenario in the present day with giant companies like SpaceX and Blue Origin competing to pioneer space exploration [1][2]. While this technology is fascinating, it has been growing for decades [3]. However, modern rocketry became more pronounced in the 20th Century [4]. Robert H. Goddard, an American, conducted experiments with solid and liquid rocket propellants. He managed to fly a liquid-propelled rocket to an altitude of 12.5 meters in 1926 [5]. Jack Parsons, an American aerospace engineer in 1942, invented modern solid rocket propellant rockets [6]. He substituted double-base propellant with asphalt and potassium perchlorate. Most recently, these propellants have been used in orbital space flights and as boosters on rockets.

Our rocket development team, the *Nakuja project*, seeks to build a low altitude solid motor propellant rocket to fly it to an altitude of 50 m. Because solid rocket motors are safer to work with and can last longer without degradation, they were the appropriate choice for this research. In this study, we conduct simulations to find out the appropriate mixtures and grain size to be cast in the solid rocket motor.

Based on the parameters obtained from the simulation, we design and cast the solid rocket motor. To enhance the motor performance, we also fabricate the nozzle. Finally, we test and analyze the propellant's performance.

2. Simulation

The simulation was conducted to visualize some abstract concepts, generate design parameters, create step-by-step progression for iterative design as well as generate safety guidelines. Autodesk Inventor was used to model casing design and material analysis [9]. This was done by utilizing the finite element analysis feature of Autodesk Inventor. There was a need to strike a balance between weight and strength. The propellant performance was simulated using OpenMotor with the parameters shown in Table I. The set parameters resulted in a nozzle cross section as shown in Fig. 1.

Table I
Simulation SETTINGS FOR Openmotor

Parameter	Value

Throat Diameter	10 mm
Exit Diameter	22 mm
Efficiency	0.85
Divergence Half Angle	15 degrees
Convergence Half Angle	35 degrees
Throat Length	5 mm
Slag Build-up coefficient	0 (m•Pa)/s
Throat Erosion coefficient	0 m/(Pa•s)
Expansion Ratio	4.84

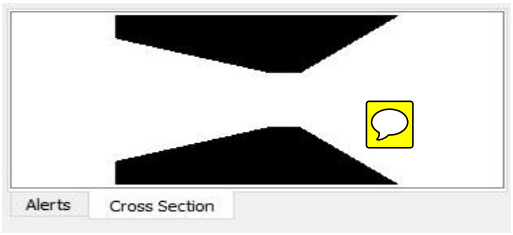

Fig 1. Nozzle cross-section designed by OpenMotor

The parameters of the propellant shown in Table I include propellant grain length, grain diameter, and combustion chamber diameter. A variation of these parameters outlined the iterative construction and testing path. The output of OpenMotor is a curve of the instantaneous thrust against time as shown in Fig. 2. This data coupled with the initial weight of the motor and propellant are combined to form a .eng file. This file can be used with OpenRocket to simulate rocket flight.

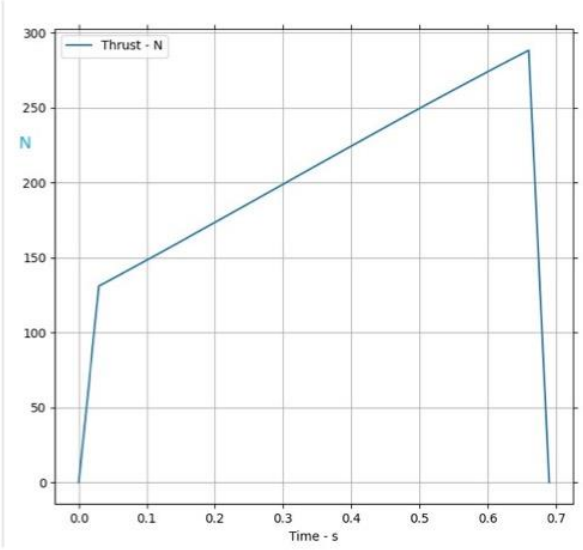

Fig 2. Thrust curve generated by OpenMotor

The various motor configurations developed throughout the iterative design process are illustrated in Table II.

Table II
Imported .eng files from openRocket

Designation	Total Impulse (Ns)	Diameter (mm)	Length (mm)
F87	63	40	200
F46	70	40	70
F94	71	40	200
F65	73	40	200
F64	75	40	200
G47	86	40	90
G146	110	40	200
G108	110	40	200
G106	115	40	200
G152	119	40	200
G168	121	40	200
G117	131	40	200
G114	133	40	200
G186	140	40	200

Fig. 3 shows the simulated positioning of the motor inside the rocket during simulation.

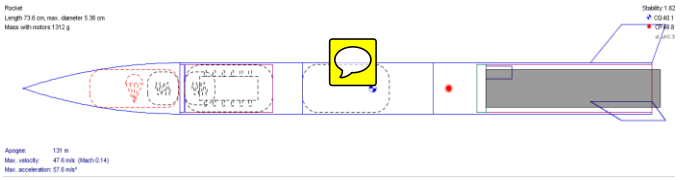

Fig. 3. Image of rocket with the motor in place

The results from simulations conducted are highlighted in Table III. The parameters that were critical to development are the apogee and time of flight.

Table III
Simulation results from OpenRocket

Name	Apogee (m)	Time of flight (s)
V6- KNSU	107	37.2
V6-KNSU-nozzled	358	114
V7-KNSU	134	45.4
V7-KNSU-nozzled	450	142
V8-KNDX	137	46.6
V8-KNDX-nozzled	401	127
V9-KNDX	134	45

3. Design

During iterative testing and development, the geometry of the motor changed. The initial motor design was as illustrated in Fig. 4.

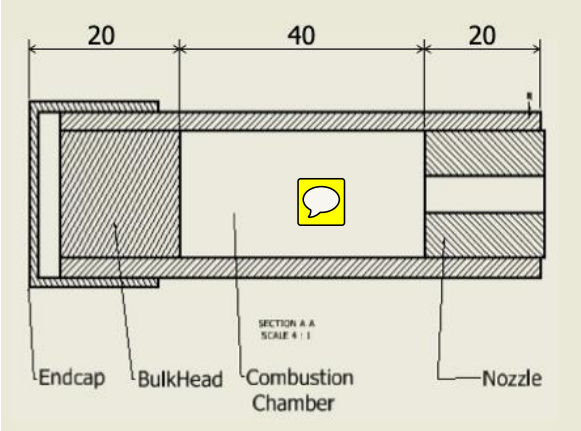

Fig. 4. Initial motor design

The final design of the motor was as illustrated in Fig. 5.

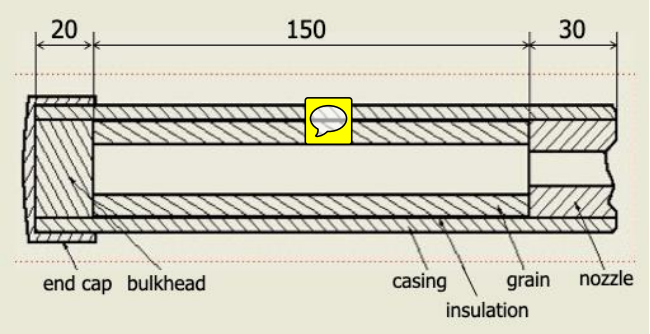

Fig. 5. Final motor design

The different parts of the motor design can be broken down as follows.

Casing

This part forms the body of the motor and is hollow to accommodate the propellant grain and the nozzle. The casing has some functional requirements, which include; it should be able to withstand the high temperatures and pressure of propellant combustion and it should be lightweight. The non-functional requirements of the casing include that it should be locally available and should be cheap to facilitate iterative testing. The research was conducted on several materials and two were shortlisted (i.e., Aluminum and PVC). They both met the design requirements but PVC was chosen, as it was cheaper, more readily available, and easier to work with. The first iterations of the motor used ¾-inch PVC pipe of various lengths. The length of the final motor casing was chosen to be 200 mm. The PVC pipe used was PN25 meaning it has a pressure rating of 2.5 MPa. The pipe had an outer diameter of 40 mm and an inner diameter of 31 mm. The length of the propellant grain heavily influenced this length. The hollow tube would be capped by a PVC fitting called an end cap and some hydraulic cement forming the bulkhead. The other end of the hollow tube would house the nozzle.

3.1 Propellant

The research was conducted and the team settled on three possible propellants for development. All the propellants had a simple combination of oxidizer, fuel, and catalyst. For all the three propellants Potassium Nitrate was chosen as the oxidizer and Iron III oxide was chosen as the catalyst. Potassium Nitrate was chosen because of its fair performance and availability. The three propellants chosen were; 1. Potassium Nitrate and Sucrose (KNSU) 2. Potassium Nitrate and Dextrose (KNDX) 3. Potassium Nitrate and Sorbitol (KNSB). The oxidizer to fuel ratio for all three fuels was 65 to 35. Meaning that the propellant was oxidizer rich to ensure that all the fuel was burnt during combustion.

3.2 Nozzle

Two nozzle designs were settled upon during the design of the motor.

a) Simple straight nozzle

This nozzle has a simple construction as the diameter of the throat is uniform throughout the length of the nozzle as illustrated in Fig 6.

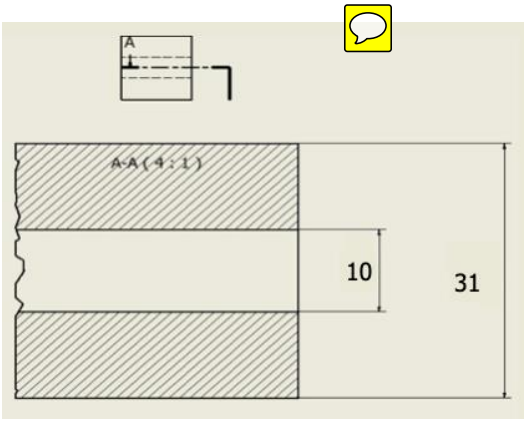

Fig. 6. Simple straight nozzle

b) de Laval nozzle

This nozzle consists of a converging section, throat, and diverging section as illustrated in Fig. 7 [10].

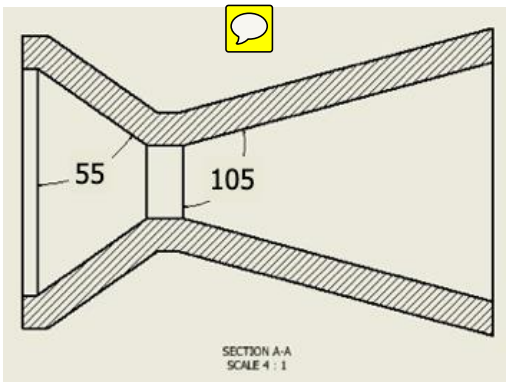

Fig. 7. Simple de Laval nozzle

The converging section of the nozzle causes the gases produced during combustion to accelerate linearly towards the throat. At the throat, the gases achieve sonic velocity and in the diverging section, the pressure of the gases is reduced while conversely increasing the velocity of the gases.

c) Nozzle CFD Analysis

A two-dimensional CFD analysis was carried out for the nozzle design. From the resulting contours a symmetry model was generated. Double precision was used with 2 parallel processors selected. The solver type was density-based and the flow was set to axisymmetric. The energy equation was turned on and the viscous model was set to k-epsilon (k-ϵ). To simulate a turbulent flow k-ϵ (Realizable) viscous model is used. The properties of the working fluid are stated in Table IV.

Table IV
Properties of Air

Property	Air
Density	Ideal Gas
Specific Heat	1006.43 (J/kg.K)
Thermal conductivity	0.0242 (W/m.K)
Molecular Weight	28.966 (kg/kmol)
Viscosity	Sutherland

The boundary conditions used are shown in Table V.

Table V
Boundary Conditions

Property	Value
Pressure inlet total gauge pressure	2268000 (Pa)
Initial gauge pressure	2267000 (Pa)
Inlet temperature	1200 (K)
Pressure of operating conditions	0 (Pa) (absolute)
Outlet pressure, Temperature	39365 (Pa), 243 (K)

A structured mesh was generated for the profile resulting in 2587 nodes and 2410 elements. Face meshing was applied on each of the five subsections with adaptive sizing and a resolution of 7. The resulting mesh is shown in Fig. 8.

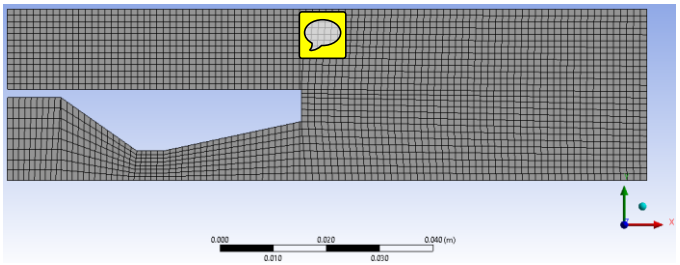

Fig. 8. Nozzle mesh

The pressure contours generated are in Fig. 10. The model used was k-ϵ. For gas, the pressure obtained for the k-ϵ is 11.5% higher than the theoretical value [12].

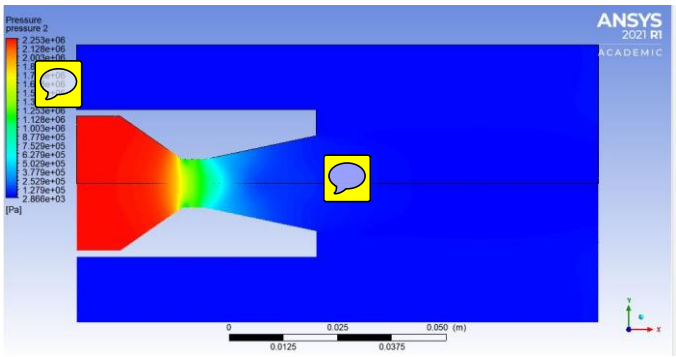

Fig. 9. Pressure contour

From the results in Fig. 9, it was observed that the pressure decreases from the convergent side of the nozzle and no shocks are observed to form in the nozzle which was ideal.

The contours generated for the velocity are shown in Fig. 11. For Air velocity obtained in k-ϵ model, it is 2.5% lower than the theoretical value [12].

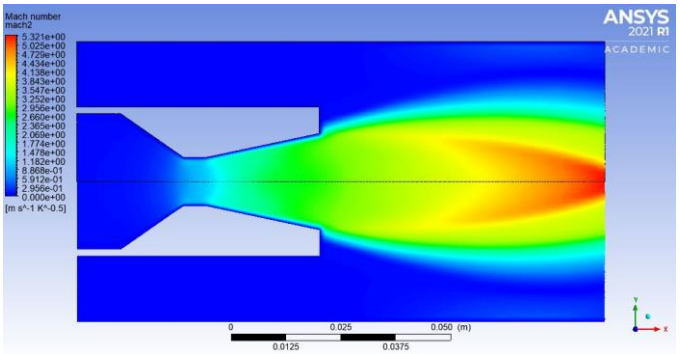

Fig. 10. Mach number contour

The Mach number of the fluid as shown in Fig. 10 increases along the length of convergent-divergent nozzles due to conservation of momentum in the fluid.

4. Fabrication

4.1 Casing

The casing was fabricated as follows: From V1 to V5 (earlier versions of the motor) the casing was made by cutting to size a 3/4 inch PVC pipe. The length of the pipe varied depending on the required geometry of the specific motor. For later versions, the PVC pipe used had an outer diameter of 60 mm with the length of each being cut at 200 mm. The cut ends were smoothened and squared using sanding paper.

4.2 Propellant

During the development, alterations were made to the method of preparing the propellant. The process started by obtaining the fuel and oxidizer. For sucrose we used icing sugar as the particles are very small, for dextrose we used glucose (dextrose monohydrate) and sorbitol was obtained as sorbitol 70% solution. Potassium Nitrate was obtained with a purity of 99% from local chemical suppliers. Iron III oxide was obtained from a chemical supplier at 99% purity. To obtain solid sorbitol from the solution, the sorbitol solution was heated in a pan using an electric heater for 15 minutes at 150 degrees Celsius.

The weight of the required propellant was obtained from OpenMotor. The solid components were first blended using a blender and sieved to obtain the finest particles. They were then weighed out using an electronic scale and mixed in the ratio stated above (65:35; O: F) the catalyst was added as 1 % of the oxidizer and fuel mixture. The mixture was placed in a plastic can and shaken vigorously. For sorbitol, the solid obtained was in the form of a slurry and was used as-is.

The first iterations of propellant development involved dry packing this propellant mixture into the casing using a mallet and a wooden rammer. The propellant mixture was added in small amounts into the casing and each time it was packed in using the rammer and the mallet. When the desired height of the propellant was achieved, a drill bit was used to create a combustion chamber. The size of the combustion chamber depended on the required grain geometry.

For further motors, the propellant grain was prepared by casting. Casting involves heating the propellant mixture until it melts and pouring it into a mold to obtain the desired shape. The grain is left to solidify and then removed from the casting apparatus. The casting process was done using an electric heater, a pan, and coring rods and tubes. A coring rod is a cylindrical piece of metal with a chosen size all through. A coring tube is made by cutting 150 mm of PVC pipe and then lining the inside with cardboard paper. The paper serves as a cover for the solid propellant as well as an insulator to the casing during combustion.

The casting process began by preheating the pan and then adding about half the propellant mixture to the pan. Using a wooden spoon, the mixture was stirred until it started to melt. More of the mixture was added at this point. The propellant was heated to a casting temperature of 145 °C for KNSU, 135 °C for KNSB and KNDX. The propellant was then poured into the casting tube and the coring tool was inserted to make a combustion chamber. The coring tool was left in for a sufficient time; 3 minutes for KNSU, 10 minutes for KNDX, and 20 minutes for KNSB; until the propellant began to solidify. At this point, the coring tool was removed and the grain was left to cool in a desiccator. The desiccator was constructed using a simple lunch box in which a sufficient amount of Fused calcium chloride was placed.

The grain was left to cool until it was fully solidified. For KNSU it would take roughly 3 hours, for KNDX it would take about 24 hours and for KNSB it would take 48 hours Once the grain had solidified it was ready for firing. An image of the casting process is illustrated in Fig 11.

Fig. 11. Casting process

The final grain obtained was red for all three propellant types as a result of the Iron III oxide. Fig. 12 shows the grain in the casting tube and casting case after removing the coring rod.

Fig. 12. Cast grain

4.3 Nozzle

Both the straight and de Laval nozzles were made using

hydraulic cement. The cement is fast setting and only requires to be mixed with water.

a) Straight nozzle

The straight nozzle was constructed by placing a finite amount of cement into an open end of the cut PVC pipe and letting it solidify. A drill bit was then used to make a hole of the required diameter in the cement.

b) de Laval nozzle

This nozzle was first made by painting the inside of the casing with acrylic paint. This is done to enhance the cohesion of the hydraulic cement and the walls of the PVC pipe. The paint was allowed to dry overnight. The converging side was made using a 3D printed part displayed in Fig. 13.

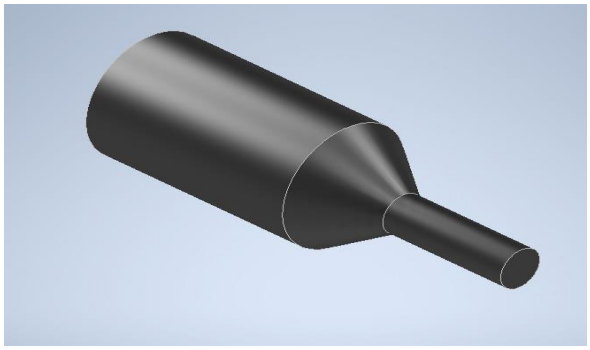

Fig. 13. 3D printed part used to fabricate the nozzle

The cement was first mixed with water. The part was pushed in through the unpainted side until the tip of the part was flush with the painted end of the pipe. The cement was then poured onto the cavity formed and then allowed about 3 minutes to solidify. The piece was then forced out using a screwdriver and a hammer. The diverging side was made by using a scraper to remove the cement until the required angle of 15 degrees was obtained. The completed nozzle was as shown in Fig. 14.

Fig. 14. Fabricated de Laval nozzle
(left: diverging side, right: converging side)

4.4 Assembly

The assembly of the motor was done by first constructing the nozzle as described above. The grain obtained after casting was placed in the casing with the constructed nozzle. The open end of the casing was then sealed with hydraulic cement. To reinforce this a PVC end was added. The PVC end cap is a PVC fitting of an internal diameter of 40 mm and an external diameter of 50 mm. The end cap was attached using PVC tangit glue. The external surface of the casing was buffed using sandpaper and the ends were made square. Tangit glue was applied to the casing and the internal side of the end cap. The two were then assembled and held in position tightly for about one minute. The assembly was left to cure for about two hours before any firing could take place. The assembly was as illustrated in Fig. 15.

Fig. 15. Side view of the assembled motor

5. Testing

Testing was conducted to generate the motor thrust curves. Testing was conducted in the form of static firing tests. The tests were conducted using a vertical static fire test stand fabricated from mild steel due to its high dynamic yield strength under high-velocity impact [8]. The thrust measurement apparatus consisted of four pin-load cells in a Wheatstone Bridge circuit with a maximum load capacity of 200 kilograms, an HX711 load cell amplifier with a sampling frequency of 80 Hz, and a 10-bit A/D converter of Arduino. The unit used a bench vice to hold the motor in place with the load cells mounted on mild steel bars below the bench vice. The system was calibrated using a reference weight. The test stand assembly is shown in Fig. 16, the data collection pipeline in Fig. 17, and the remote ignition system in Fig. 18.

Fig. 16. Static fire test stand assembly with solid rocket motor

Fig. 17. Diagram of data collection

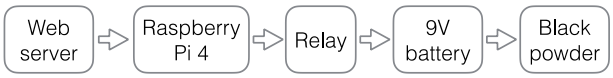

Fig. 18. Test stand remote ignition sequence

The remote ignition system consisted of an igniter placed through the nozzle of the motor reaching the combustion chamber. The purpose of the igniter was to convert an electrical signal from the 9V battery to heat which would ignite the propellant in the motor. The igniter we used for testing consisted of nichrome wire, 10 mm diameter straws, and black powder shown in Fig. 19. One end of the straws was sealed using hot glue. The straw was then filled with black powder. Nichrome wire with leads attached to it was then placed in contact with the black powder. This was done carefully so that the nichrome was in contact with the black powder but did not short itself or the lead wires.

Fig. 19. Igniters

6. Results

Prototype motors

The first set of motors were 4 variations of the same grain diameter and grain length with variations in the core diameter.

The 4 motor variants had 2 propellant compositions: KNDX and KNSU. The variation between them was different core diameters to explore the effect of chamber pressure on motor performance. The KNSU motors were designated V7 and V8 while the KNDX motors were designated V9 and V10. The thrust curves of V6 and V7 are as shown in Fig. 20. The V9 and V10 variants of the propellant failed to ignite during the static firing test and thus could not be evaluated.

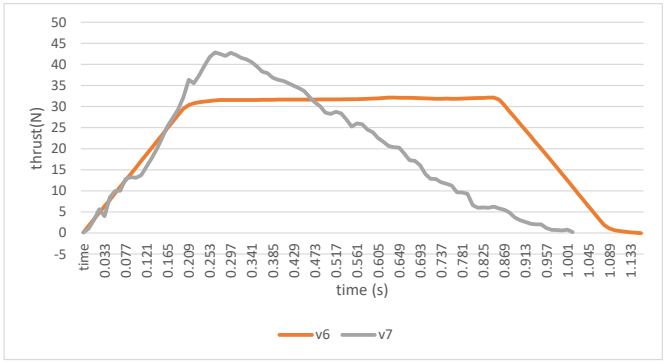

Fig. 20. V6 and v7 thrust curve

Final Motor

Improvements were made to the V7 prototype motor to include a nozzle to optimize motor performance as shown in Fig. 21.

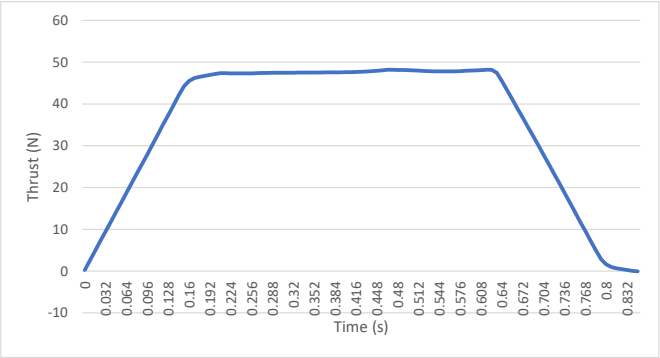

Fig. 21. Thrust against time

7. Discussion

From the graph in Fig. 20, it is observed that v6 maintains a neutral ideal curve while V7 has a high peak followed by a rapid drop in thrust. This occurred in V7 as during the static firing test a failure occurred in the bulkhead leading to a drop in chamber pressure thus the observed drop in performance. It was however noted that V7 developed a higher peak thrust of 43 N. V7 also had a specific impulse of 156.68 s compared to v6, 155.94 s respectively. The total impulse for V6 and V7 was 28.07 N-s and 23.50 N-s respectively. Total impulse is given by (1).

$$I_t = \int_0^t F\,dt \tag{1}$$

In (1), *It* (N-s) is the *total impulse* that is given by the integral of the *thrust F* (N) over the operating period of the motor (s). A delivered specific impulse is given by the total impulse divided by the propellant mass.

Final Motor

The peak thrust generated was 48 Newtons, with a total impulse of 31.32 N-s and a specific impulse of 164.82 s, and an average thrust of 35.09 N.

Propellant Comparisons

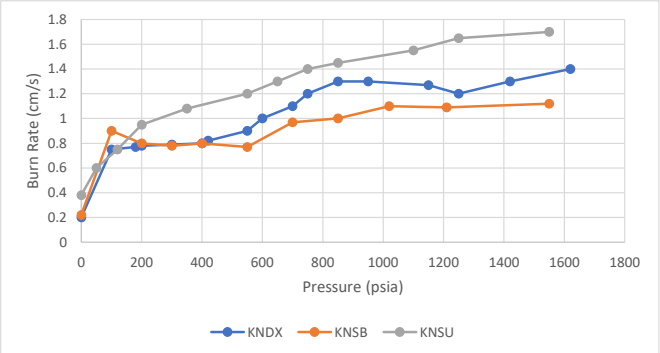

Fig. 22. Burn rate for different propellants (adapted from [11])

From the graph in Fig. 22 and experiments carried out it was observed that KNSU had a higher burn rate but resulted in higher pressures which were a safety concern in case of a catastrophic failure. KNDX was considered as an alternative but it proved difficult to store due to its hygroscopic nature. KNSB was left out as sorbitol was not readily available in the given time constraints but will be explored in future developments. An additional advantage that KNDX and KNSB had over KNSU was that they had lower casting temperatures. As a result, KNDX and KNSB are easier to handle during casting and remain fluid for a longer time.

Performance Improvement

An important takeaway was the overall incremental performance of the rocket motor for the static tests carried out. This is best characterized by the comparison between the actual and simulated peak thrust as shown in Fig. 23.

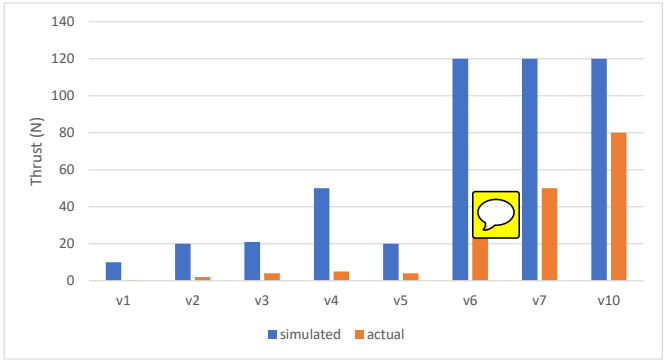

Fig. 23. Comparison of actual and simulated thrust

The versions V1-V5 differ in size to the V6-V10 hence the difference. The propellants in V1-V5 also don't include a catalyst (Iron oxide) in their formulation. For V6-V10, the grain length is the same as well as other factors only differing in V10 which had a different nozzle. V1-V5 were used to test the viability of fuel used and were set aside for latter versions to improve on performance.

A key factor in improving performance between V6 and V10 was the improvement in grain density. During static tests, it was noted that the simulated grain mass did not match up to the actual value. This would result in a lower performance than expected. This might have resulted from gas porosity during the pouring stage of casting. This was solved by improving compacting during the pouring stage of casting by ramming the molten propellant to fill up available space and expel trapped gases.

Propellant mixing processes were also enhanced to bring about increased performance. The propellants were sifted to remove large particles after being

ground using a blender. Dry mixing was also enhanced with shaking in a container for extended periods. Smaller particles and close mixing meant that the oxidizer and fuel had closer contact resulting in a more effective reaction.

The V10 and V7 differ in the nozzle utilized. The convergent-divergent nozzle developed brought about increased performance due to the increased velocity of exhaust gases due to pressure reduction from the converging side of the nozzle to the diverging as a result of energy conservation. This resulted in improved performance compared to the straight nozzle initially used.

8. Conclusions

By analyzing the thrust curves obtained from the static fire tests of KNSU and KNDX, this study established that for a given mass of solid rocket motor propellant, KNSU generated more thrust and demonstrated a higher burning rate compared to KNDX. However, KNDX has a bigger safety margin compared to KNSU because of its lower chamber pressure. Additionally, analysis results showed that grain inclusions, in particular, air bubbles, negatively influence the thrust performance of both KNSU and KNDX. Concerning the propellant development method, tests on the propellants considered in this study showed that dry heating produces a homogenous grain structure. The post-burning analysis showed better combustion efficiency of KNSU compared with KNDX. The important role of catalysts has been shown. In particular, the addition of Iron (III) oxide during the casting process resulted in a significant increase in the burn rate and the amount of burned propellant for both sucrose and dextrose-based propellants.

Future research into solid rocket motor propellants for model rockets should focus on determining ways of optimizing the performance of sugar-based rocket propellants such as KNSU and KNDX by for example using additives. There is also a need to replace KNO_3 with high-performance biodegradable oxidizers and minimize plastic deformation of the PVC casing during combustion. Additionally, while this paper examines the performance of KNSU and KNDX rocket propellants, further experimental and observational studies are required to gain more insight into the factors affecting the performance of KNDX and KNSU propellants.

Acknowledgement

The authors thank Jomo Kenyatta University of Agriculture and Technology for the use of the Integrated Prototyping and Innovation Center. The authors also acknowledge the financial support of the AFRICA-*ai*-JAPAN Project (JICA) and the technical support of Mr. Ben Maniafu.

References

[1] M. Vozoff and J. Couluris, "SpaceX products-advancing the use of space," in *AIAA SPACE 2008 conference & exposition*, 2008, p. 7836.

[2] J. T. Smith, "The Future of Space Exploration: SpaceX's Petitions for Inter Partes Review against Blue Origin's Rocket-Landing Technology," *SMU Sci. & Tech. L. Rev.*, vol. 19, p. 65, 2016.

[3] L. T. DeLuca, "Highlights of solid rocket propulsion history," in Chemical Rocket Propulsion, Springer, 2017, pp. 1015–1032.

[4] D. A. Singh, "Sugar Based Rocket Propulsion System-Making, Analysis & Limitations," vol. 2, no. 5, p. 8, 2015.

[5] S. Helmy and A. Helmy, "The Origins and Growth of Short Range Liquid Propellant Ballistic Rockets," in AIAA Propulsion and Energy 2020 Forum, 2020, p. 3792.

[6] P. Umholtz, "The history of solid rocket propulsion and Aerojet," *35th Joint Propulsion Conference and Exhibit*, 1999.

[7] W. R. Dornberger, "The German V-2," Technology and Culture, vol. 4, no. 4, pp. 393–409, 1963.

[8] M. Singh et al., "Dynamic yield strength of mild steel under impact loading," Defence Science Journal, vol. 58, no. 2, p. 275, 2008.

[9] L. A. N. Wibawa, K. Diharjo, W. W. Raharjo, and B. H. Jihad, "Stress Analysis of Thick-Walled Cylinder for Rocket Motor Case under Internal Pressure," *Journal of Advanced Research in Fluid Mechanics and Thermal Sciences*, vol. 70, no. 2, Art. no. 2, 2020.

[10] N. K. Mishra and D. S. S. Prasad, "MODELING & SIMULATION OF ROCKET NOZZLE," vol. 2, no. 2309, p. 8, 2014.

[11] 'Richard Nakka's Experimental Rocketry Web Site'. https://www.nakka-rocketry.net/sorb.html (accessed Jul. 12, 2021).

[12] V. A. Hemanth and U. S. Jyothi, 'CFD Analysis of a Solid Propellant Retro Rocket Motor using Ansys Fluent', in *E3S Web of Conferences*, 2020, vol. 184, p. 01054.187(2), pp. 507-516, 2001.